Supporting Information

Reactive Intermediates or Inert Graphene? The Temperature and Pressure Determined Evolution of Carbon in the CH_4–Ni(111) System

*Kaidi Yuan[1,2], Jian-Qiang Zhong[3], Shuo Sun[2], Yinjuan Ren[4], Jia Lin Zhang[4], Wei Chen[1,2,4]**

1 National University of Singapore (Suzhou) Research Institute, 377 Linquan Street, Suzhou Industrial Park, Jiangsu 215123, China

2 Department of Physics, National University of Singapore, 2 Science Drive 3, 117542, Singapore

3 Center for Functional Nanomaterials, Brookhaven National Laboratory, Upton, New York 11973, United States

4 Department of Chemistry, National University of Singapore, 3 Science Drive 3, 117543, Singapore

Corresponding Author

Associate Professor Wei Chen: phycw@nus.edu.sg

1. Carbon coverage estimation

Table S1 shows the estimated coverage of carbon species of **Figure 1** in the main text. The calculation of "Normalized Area" is obtained through dividing the peak area by the background level and FWHM. The coverage (per Ni atom) is calculated through dividing the "Normalized Area" by 6.0, a factor obtained on the basis that the fully covered graphene (2 carbons per surface Ni) has the "Normalized Area" of 12.

Figure 1 of the main text

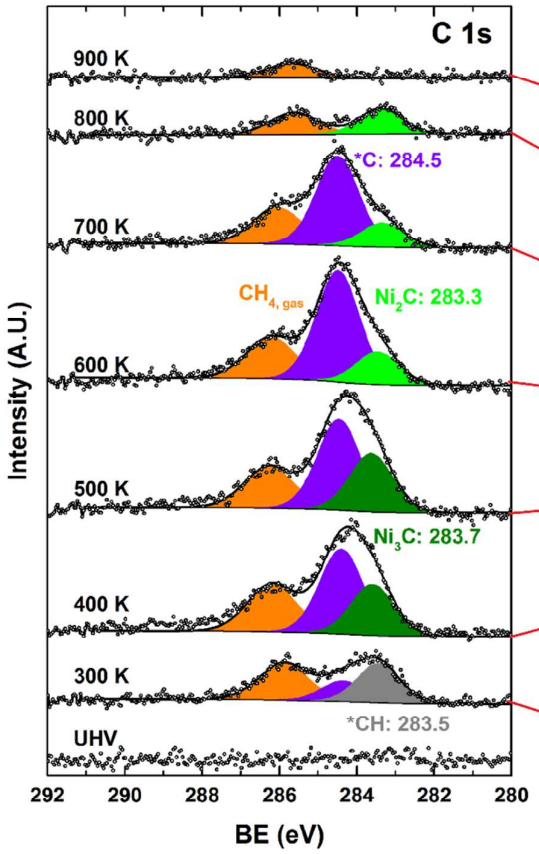

Table S1: Carbon Coverage Estimation

Temperature	Species	Normalized Area	Coverage (per surf. Ni)
900 K	Gas	0.81	--
800 K	Gas	1.19	--
	*C_n	0.24	0.04
	Ni_2C	1.35	0.22
700 K	Gas	1.97	--
	*C_n	4.79	0.80
	Ni_2C	1.32	0.22
600 K	Gas	2.14	--
	*C_n	5.78	0.96
	Ni_2C	1.67	0.28
500 K	Gas	2.14	--
	*C_n	4.74	0.79
	Ni_3C	2.99	0.50
400 K	Gas	2.16	--
	*C_n	3.89	0.65
	Ni_3C	3.13	0.52
300 K	Gas	1.94	--
	*C_n	1.02	0.17
	*CH	2.19	0.37

2. Ni 2p peak of clean and graphene-covered Ni(111)

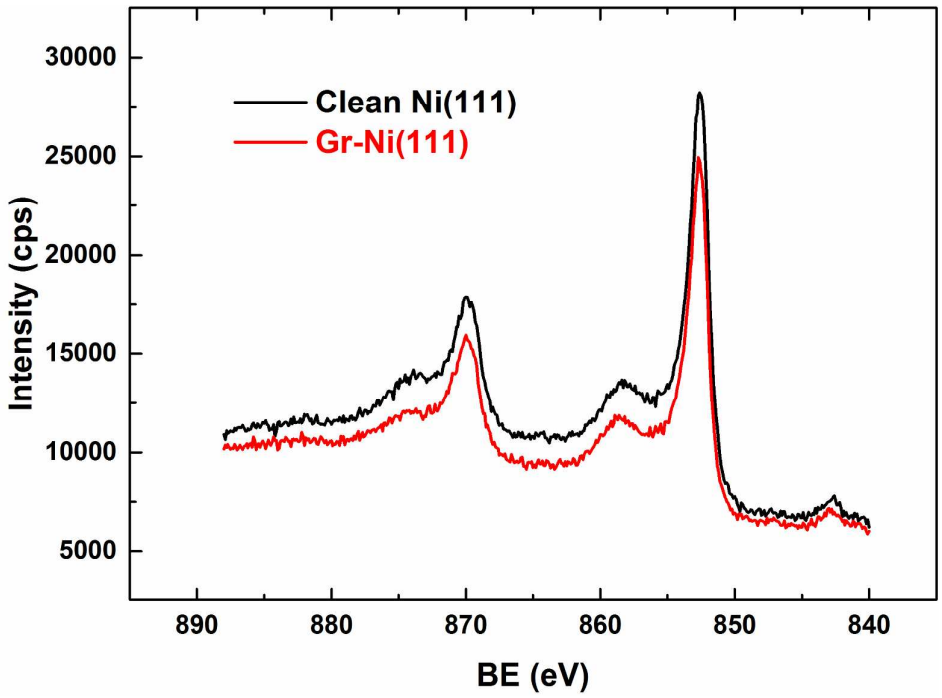

Figure S1. Ni 2p spectra of clean (black) and graphene covered (red) Ni(111). Both of them were measured in UHV, before CH_4 dosing or after the evacuation of CH_4.

3. LEED Simulation for the clock reconstructed Ni_2C

LEED simulation of the Ni_2C structure was obtained by software "LEEDpat version 4.1". A reflection symmetry was added by compositing the flipped image to the originally simulated image where only the 3-fold domains were considered.

Two typical description of the Ni_2C from literatures are presented here, with the Wood's notations, vector length and the angle against the Ni(111) base vectors. These two expressions have very little difference in the actual parameters of the Ni_2C: a unit lattice of about twice of the Ni–Ni distance in Ni(111), and the angle of about 2.6˚ and 94.1˚ against the Ni–Ni direction. The simulated diffraction patterns are close to the measured pattern as shown in **Figure S2**.

Nature 1969: $\sqrt{39}R16.1° \times \sqrt{39}R16.1°$; from Ref. 1

a = 4.98 Å = 2.00 $\mathbf{r}_0$, b = 4.86 Å = 1.95 $\mathbf{r}_0$,

γ = 94.1˚, θ = 2.6˚

ACSNano2012: $\sqrt{39}R16.1° \times \sqrt{37}R - 34.7°$; from Ref. 2

a = 4.86 Å = 1.95 $\mathbf{r}_0$, b = 5.06 Å = 2.03 $\mathbf{r}_0$,

γ = 94.72˚, θ = 2.83˚

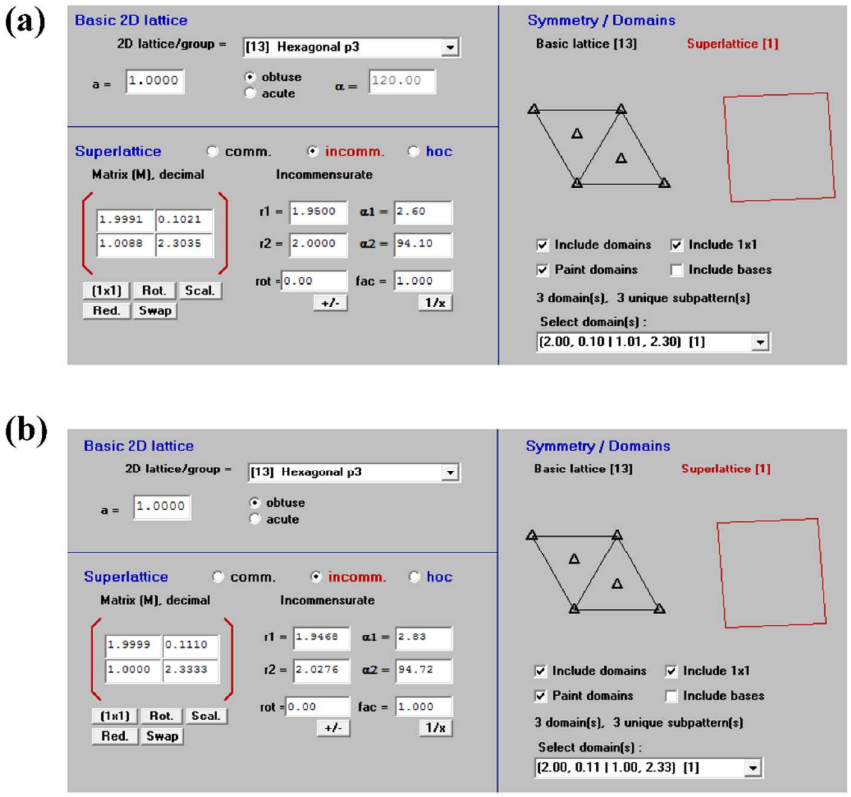

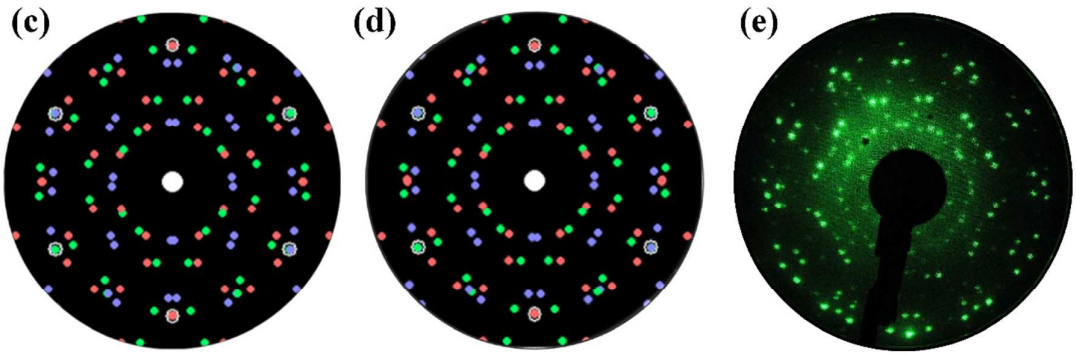

Figure S2. Parameters (a, b) and simulated LEED patterns (c, d) of the clock-reconstructed Ni_2C on Ni(111) from Reference 1 and Reference 2, respectively. The measured pattern in (e) was obtained at 70 eV beam energy.

4. Schematic drawing of inclined C–H bond, an explanation to the LEED pattern of the *CH adsorbates.

The ring-like $\sqrt{3} \times \sqrt{3}$ LEED pattern of the sample after CH_4 exposure at 300 K was inferred from the inclined C–H bond, as shown in Figure S3. The reason for the ring-type diffraction (rather than spots) was inferred from the non-perpendicular C–H bonds with a (probably) fixed zenith angle and randomly distributed azimuth angles. For the 70-eV electron beam, the angle between the (01)–beam and the z-axis is ~42.8˚. By comparing the diameter of the diffraction ring to the (01) vector of Ni(111), the effect zenith angle of the C–H bond was estimated as 8.7˚.

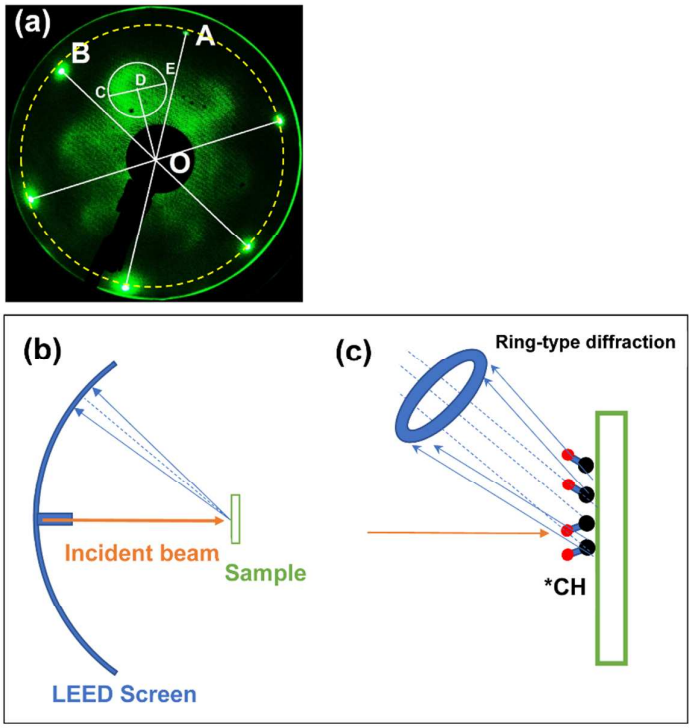

Figure S3. (a) Measured LEED pattern after CH_4 exposure at 300 K; (b, c) Schematic explanation of the formation of ring-like

For the 70 eV electron beam, its wavelength can be calculated using the De Broglie formula:

$$\lambda = \frac{h}{p} = \frac{6.62607\times10^{-34}\ \text{J·s}}{\sqrt{2E\cdot m_e}} = \frac{6.62607\times10^{-34}\ \text{J·s}}{\sqrt{2\times70\ eV\cdot 9.10938356\times10^{-31}kg}} = 1.466\times10^{-10}\text{m}$$

Knowing that the Ni–Ni distance of 2.49×10^{-10} m, the angle between the (01) diffraction beam of Ni(111) and the normal ***n***, can be calculated:

$$\lambda = d \cdot \sin(\theta) = \frac{2.49\text{Å}\times\sqrt{3}}{2} \cdot \sin(\theta) = 1.466\,\text{Å}$$

$$\Rightarrow \angle nOA = \theta = 42.8°,$$

$$\frac{2.49\text{Å} \times 3}{2} \cdot \sin(\angle nOD) = 1.466\,\text{Å}, \Rightarrow \angle nOD = 23.1°$$

The measured CD:DO in panel (a) is 1:2.66. Therefore, the $\angle COD$ is about 8.7˚, indicating that the C–H bond has deviated ~8.7˚ (effective) from the normal.

5. O_2 probing test on the nickel surfaces covered by pre-treated carbon species

The clean Ni(111) was first exposed to 0.4 mbar CH_4 at various temperatures (300–900 K). After cooling to room temperature and evacuating to UHV, it was characterized by UPS. Then 1×10^{-7} mbar O_2 was introduced, and the UPS characterization continued. **Figure S4** (a–e) show the time-resolved UPS spectra. The reduce of d-band electronic state near Fermi Edge, and the increase of O 2p are the general feature during the O_2 exposure. In panel (f), the intensity at 0.168 eV binding energy was plotted as a function of O_2 dosage. The *CH covered sample (300 K) showed delayed oxidation, while others were oxidized immediately after O_2 dosing. This reflects the reactivity of carbon species (*CH, Ni_3C, $*C_n$ and Ni_2C) towards O_2. It is noted that the sample after 400 K CH_4 dosing were characterized by LEED prior to the O_2 dosing. The UPS spectra shrank after electron beam bombardment, and the initial oxidation rate of the 400 K sample became slower. For the graphene covered sample, no change in the valence band was observed, and therefore are not shown here.

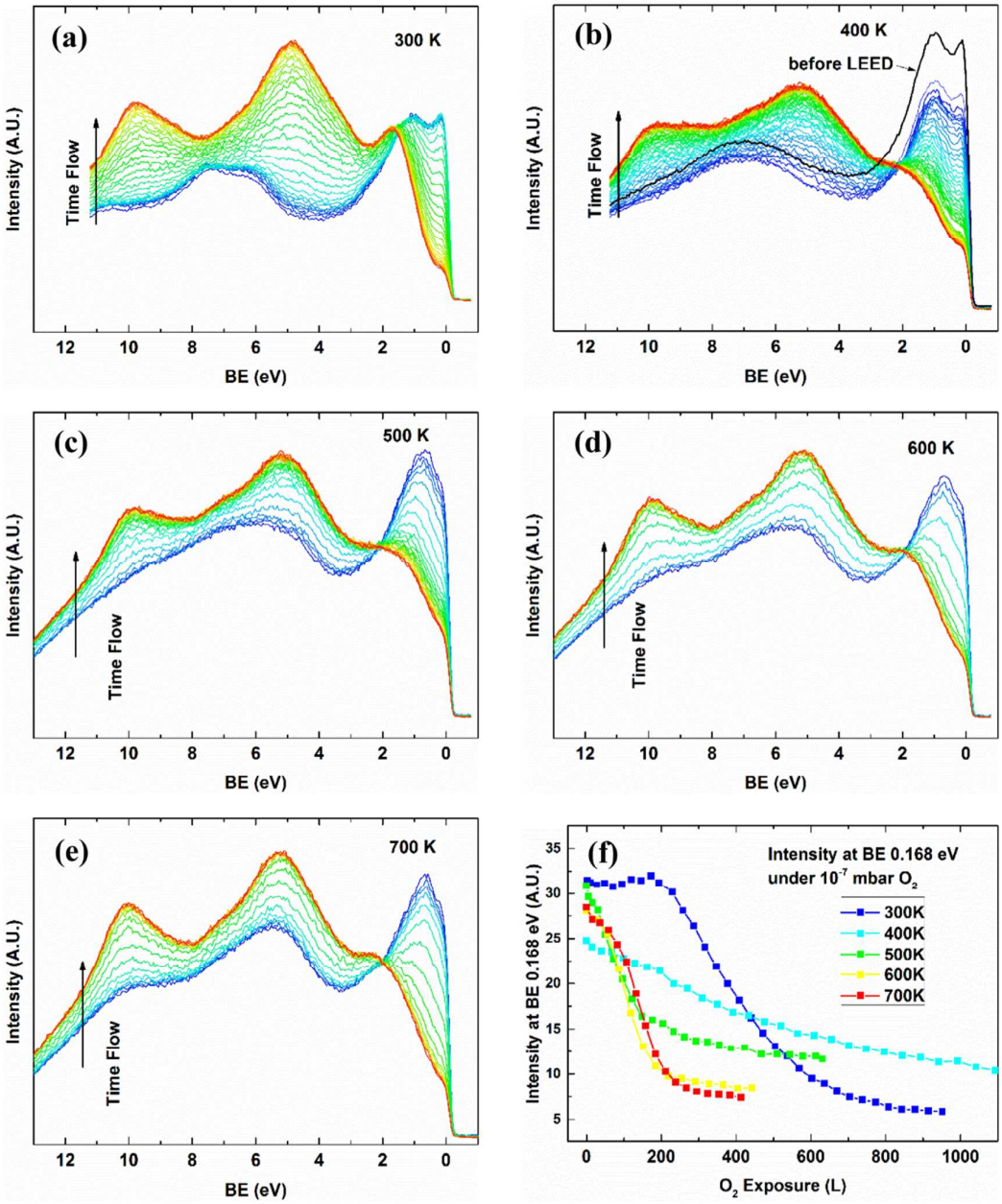

Figure S4. (a–e) Time resolved UPS spectra during O_2 dosing in 1×10^{-7} mbar O_2, at 300 K, after CH_4 pre-treatment at various temperatures. (f) The intensity at the binding energy of 0.168 eV below Fermi Edge, plotted against the O_2 dosage in Langmuir.

6. Comparison of activation energies for CH_4 dissociation on Ni(111)

Table S 2 lists the reported activation energies and sticking probabilities (in black) for CH_4 on Ni(111). For easier comparison, they were converted to the sticking probability at 300 K or activation energy **in bold (conv.)** using the following equations:

$$S(T) = e^{-E_a/k_B T}$$

Table S2. Some reported activation energies for CH_4 dissociation on Ni(111).

Apparent E_a (eV)	Sticking Probability	Remarks	Ref. (Year)
0.879 (conv.)	4×10^{-8} at 600K **1.7×10^{-15} at 300 K (conv.)**	1.33 mbar, bulb experiment (uneven heating might exist)	3 (1991)
0.546	**6.7×10^{-10} at 300K (conv.)**	1.33 mbar	4 (1987)
0.767 (conv.)	**1.3×10^{-13} at 300K (conv.)** 1.3×10^{-8} at 500K (meas.)	$<10^{-2}$ mbar, using a thermal finger	5 (2002)
0.516 (conv.)	1.5×10^{-9} beam energy 0.73 eV **2.1×10^{-9} at 300K (conv.)**	Molecular beam	6 (1986)
0.718	**8.6×10^{-13} at 300K (conv.)**	Ab initial	7 (1992)
0.649 (steps) 0.859 (terrace)	2.8×10^{-7} at 500K **1.3×10^{-11} at 300K (conv.)** 2.1×10^{-9} at 500K (meas.) **3.7×10^{-15} at 300K (conv.)**	0.01 mbar, thermal finger at 500K	8 (2005)
1.31	**9.8×10^{-23} at 300K (conv.)**	DFT	9 (2012)

REFERENCES

(1) McCarroll, J. J.; Edmonds, T.; Pitkethly, R. C. *Nature* **1969**, *223*, 1260.

(2) Jacobson, P.; Stöger, B.; Garhofer, A.; Parkinson, G. S.; Schmid, M.; Caudillo, R.; Mittendorfer, F.; Redinger, J.; Diebold, U. *ACS Nano* **2012**, *6*, 3564.

(3) Hanley, L.; Xu, Z.; Yates, J. T. *Surf. Sci. Lett.* **1991**, *248*, L265.

(4) Jr., T. P. B.; Goodman, D. W.; Kay, B. D.; Jr., J. T. Y. *J. Chem. Phys.* **1987**, *87*, 2305.

(5) Egeberg, R. C.; Ullmann, S.; Alstrup, I.; Mullins, C. B.; Chorkendorff, I. *Surf. Sci.* **2002**, *497*, 183.

(6) Lee, M. B.; Yang, Q. Y.; Tang, S. L.; Ceyer, S. T. *J. Chem. Phys.* **1986**, *85*, 1693.

(7) Yang, H.; Whitten, J. L. *J. Chem. Phys.* **1992**, *96*, 5529.

(8) Abild-Pedersen, F.; Lytken, O.; Engbæk, J.; Nielsen, G.; Chorkendorff, I.; Nørskov, J. K. *Surf. Sci.* **2005**, *590*, 127.

(9) Li, J.; Croiset, E.; Ricardez-Sandoval, L. *J. Mol. Catal. A: Chem.* **2012**, *365*, 103.